Resting-brain functional connectivity predicted by analytic measures of network communication

Joaquín Goñi[a], Martijn P. van den Heuvel[b], Andrea Avena-Koenigsberger[a], Nieves Velez de Mendizabal[c,d], Richard F. Betzel[a], Alessandra Griffa[e,f], Patric Hagmann[e,f], Bernat Corominas-Murtra[g], Jean-Philippe Thiran[e,f], and Olaf Sporns[a,1]

[a]Department of Psychological and Brain Sciences, Indiana University, Bloomington, IN 47405; [b]UMC Utrecht Brain Center Rudolf Magnus, 3584 CG Utrecht, The Netherlands; [c]Division of Clinical Pharmacology, Department of Medicine, Indiana University School of Medicine, Indianapolis, IN 46202; [d]Indiana Clinical and Translational Sciences Institute, Indianapolis, IN 46202; [e]Signal Processing Laboratory (LTS5), Ecole Polytechnique Fédérale de Lausanne, CH-1015 Lausanne, Switzerland; [f]Department of Radiology, Lausanne University Hospital and University of Lausanne, CH-1011 Lausanne, Switzerland; and [g]Section for Science of Complex Systems, Medical University of Vienna, 1090 Vienna, Austria

Edited by Marcus E. Raichle, Washington University in St. Louis, St. Louis, MO, and approved November 27, 2013 (received for review August 16, 2013)

The complex relationship between structural and functional connectivity, as measured by noninvasive imaging of the human brain, poses many unresolved challenges and open questions. Here, we apply analytic measures of network communication to the structural connectivity of the human brain and explore the capacity of these measures to predict resting-state functional connectivity across three independently acquired datasets. We focus on the layout of shortest paths across the network and on two communication measures—search information and path transitivity—which account for how these paths are embedded in the rest of the network. Search information is an existing measure of information needed to access or trace shortest paths; we introduce path transitivity to measure the density of local detours along the shortest path. We find that both search information and path transitivity predict the strength of functional connectivity among both connected and unconnected node pairs. They do so at levels that match or significantly exceed path length measures, Euclidean distance, as well as computational models of neural dynamics. This capacity suggests that dynamic couplings due to interactions among neural elements in brain networks are substantially influenced by the broader network context adjacent to the shortest communication pathways.

connectome | graph theory | network theory | brain connectivity

The topology and dynamics of brain networks are a central focus of the emerging field of connectomics (1). A growing number of studies of human brain networks carried out with modern noninvasive neuroimaging methods have begun to characterize the architecture of structural networks (2–4), as well as spatially distributed components (5–7) and time-varying dynamics (8) of functional networks. Although structural connectivity (SC) is inferred from diffusion imaging and tractography, functional connectivity (FC) is generally derived from pairwise correlations of time series recorded during "resting" brain activity, measured with functional magnetic resonance imaging (fMRI). Both networks define a multiplex system (9) in which the SC level shapes or imposes constraints on the FC level. Indeed, mounting evidence indicates that SC and FC are robustly related. Numerous studies have documented strong and significant correlations between the strengths of structural and functional connections at whole-brain (2, 10–13) and mesoscopic scales (14), as well as acute changes in FC after perturbation of SC (15).

Although there is ample evidence documenting statistical relationships between SC and FC, the causal role of SC in shaping whole-brain patterns of FC is still only incompletely understood. There are numerous reports of strong FC among brain regions that are not directly structurally connected, an effect that has been ascribed to signal propagation along one or more indirect structural paths (11), or to network-wide contextual influence (16). The present paper builds on two interrelated premises. First, if SC plays a major causal role in shaping resting-state FC, then appropriately configured generative models that incorporate SC topology should be able to predict, at least to some extent, FC patterns. To this end, a number of models have been proposed, including large-scale neural mass models generating synthetic fMRI time series (11, 17, 18) as well as analytic models based on distance and topological measures (19) or attractor dynamics (20, 21). Second, the extent to which the resting-state time courses of two brain regions become temporally aligned (i.e., highly functionally correlated) should be at least partially related to the ease with which mutual dynamic influences or perturbations can spread within the underlying structural brain network.

Both premises imply that the strength of FC is related to measures of network communication. The principal communication measure applied previously in studies of brain networks is the efficiency (22), computed as the averaged inverse of the lengths of the shortest paths between node pairs. The use of this measure is based on the assumption that short paths are dynamically favored, as they allow more direct (faster, less noisy) transmission of neural signals. However, relying on path length as the sole measure of communication does not take into account how these paths are embedded in the rest of the network, which may further modulate the dynamic interactions of neuronal populations. For example, along a given path, branch

Significance

Patterns of distributed brain activity are thought to underlie virtually all aspects of cognition and behavior. In this paper, we explore the degree to which it is possible to predict such functional patterns from the network of anatomical connections that link brain regions. To this end, we use three separately acquired neuroimaging datasets recording anatomical and functional connections in the human brain. We apply several measures of network communication that are derived analytically from the brain's anatomical network. Our principal finding is that such network measures can predict empirically measured functional connectivity at levels that exceed other modeling approaches. Our study sheds light on the important role of anatomical networks and communication processes in shaping the brain's functional activity.

Author contributions: J.G., M.P.v.d.H., A.A.-K., N.V.d.M., R.F.B., A.G., P.H., B.C.-M., J.-P.T., and O.S. designed research; J.G. and O.S. performed research; J.G., M.P.v.d.H., A.A.-K., N.V.d.M., R.F.B., A.G., P.H., B.C.-M., J.-P.T., and O.S. contributed new reagents/analytic tools; J.G. and O.S. analyzed data; and J.G., M.P.v.d.H., and O.S. wrote the paper.

The authors declare no conflict of interest.

This article is a PNAS Direct Submission.

Freely available online through the PNAS open access option.

[1]To whom correspondence should be addressed. E-mail: osporns@indiana.edu.

This article contains supporting information online at www.pnas.org/lookup/suppl/doi:10.1073/pnas.1315529111/-/DCSupplemental.

points may lead to signal dispersion and hence attenuate FC, whereas local detours may offer alternative routes that amplify FC.

Here, we present an approach toward predicting FC from SC based on several analytic measures of network communication. We used sets of high-resolution SC and FC maps of the cerebral cortex, obtained from three separate cohorts of participants and acquired using different scanners and imaging protocols. First, the relationship of FC to spatial embedding and path length was explored. Next, we attempted to predict FC from SC by implementing both linear and nonlinear computational models. We then examined the capacity of several analytic measures of network communication along shortest paths to predict FC from SC, singly and in the simple form of a joint multilinear model. Our results demonstrate that analytic measures that take into account the structural embedding of short paths are indeed capable of predicting a large portion of the variance observed in long-time averages of resting-brain FC.

Analytic Measures Related to Network Communication

A variety of network-based communication processes and associated measures have been proposed (23, 24). In this paper, we focus on a set of four measures that capture various aspects of internodal interactions along the shortest path.

The SC of a parcellation of the human cortex into N regions can be expressed as an undirected weighted graph $G \equiv \{V, W\}$ formed by a set of nodes $V = \{v_1, v_2, ..., v_n\}$ and a matrix of fiber density values $W = [w_{ij}]$ with values in the range of [0,1], and with $w_{ij} = 0$ for regions i,j that are not directly connected. The strength of a node i is defined as $w_i = \sum_{j \neq i} w_{ij}$. Converting W into a matrix of edge lengths or distances $L = [l_{ij}]$ (here calculated using the matrix transforms $L = -\log(W)$ and $L = 1/W$) allows the identification of shortest paths, comprising lists of unique weighted edges, that span the minimum distance between each node pair. Once all shortest paths have been identified, their lengths can be expressed as the weighted path length D (the sum of edge lengths) and the corresponding number of steps K.

Search information quantifies the accessibility or "hiddenness" of a path linking a source node s to a target node t within the network by measuring the amount of knowledge or information needed to access the path (25–27). Originally defined for binary networks, search information depends on the node degrees along the path and represents a measure of network navigability in the absence of global knowledge. In the present context, we are interested in the search information needed to travel along the shortest path. A shortest path between a source node s and a target node t is described by the sequence of weighted edges composing it, i.e., $\pi_{s \to t} = \{w_{si}, w_{ij}, ..., w_{kt}\}$, and by the corresponding sequence of nodes $\Omega_{s \to t} = \{s, i, j, ...k, t\}$, with $|\pi_{s \to t}| = K$ and $|\Omega_{s \to t}| = K + 1$. The probability of taking the shortest path from s to t, may be expressed as $P(\pi_{s \to t}) = \prod_{i \in \Omega^*_{s \to t}} \frac{\pi^{(1)}_{i \to t}}{w_i}$, with $\pi^{(1)}_{i \to t}$ representing the first element (weighted edge) of the path $\pi_{i \to t}$ and $\Omega^*_{s \to t}$ representing the sequence of nodes excluding the target, i.e., $\Omega^*_{s \to t} = \{s, i, j, ...k\}$. Hence, assuming no degeneracy of shortest-paths in weighted networks, the information needed to access the path is denoted by $S(\pi_{s \to t}) = -\log_2(P(\pi_{s \to t}))$.

Note that, in contrast to the measure as originally introduced (22), this definition operates on weighted graphs (which in most cases prevents the occurrence of degenerate shortest paths) and does not consider preserving knowledge about the previous step. Analogous information-theoretical treatment has been also introduced to study the reversibility of causal processes (28). Weighted edges do not ensure symmetry in search information when source and target are swapped. In other words, search information of a given shortest path depends on the assignment of the source and the target. Given the lack of directionality in the SC matrices used here, we define the search information of a bidirectional shortest-path $\pi_{s \leftrightarrow t}$ as follows:

$$S(\pi_{s \leftrightarrow t}) = \frac{S(\pi_{s \to t}) + S(\pi_{t \to s})}{2}.$$

The matching index (29) is a measure that quantifies the similarity of input and/or output connections of two nodes excluding their mutual connections, here defined for undirected weighted networks as follows:

$$m_{ij} = \frac{\sum_{k \neq i,j} (w_{ik} + w_{jk}) \Theta(w_{ik}) \Theta(w_{jk})}{\sum_{k \neq j} w_{ik} + \sum_{k \neq i} w_{jk}},$$

where $\Theta(w_{ik}) = 1$ if $w_{ik} > 0$ and 0 otherwise. Extending this measure to a set of nodes comprising a path linking a source node s to a target node t captures the transitivity of the path, or put differently, the density of local detours that are available along the path. This leads to the definition of "path transitivity" as follows:

$$M(\pi_{s \to t}) = \frac{2 \sum_{i \in \Omega} \sum_{j \in \Omega} m_{ij}}{|\Omega|(|\Omega| - 1)},$$

with the edges comprising the path $\pi_{s \leftrightarrow t}$ excluded. The measure is independent of the directionality of the path and hence ensures $M(\pi_{s \to t}) = M(\pi_{t \to s})$.

Fig. 1 schematically illustrates how four measures associated with shortest paths across a network may affect the efficiency of communication between nodes and hence the expected strength of FC. First, the strength of connections along the shortest path, expressed as the weighted path length $D(\pi_{s \to t})$, is likely to impact communication efficiency (Fig. 1*A*). Second, assuming some level of signal attenuation at each step, the number of steps along the shortest path $K(\pi_{s \to t})$ is also likely to play a role in internodal communication (Fig. 1*B*). Third, communication may be affected by the accessibility of the shortest path, quantified as the search information $S(\pi_{s \to t})$ (Fig. 1*C*). Fourth, the number of ways by which signals that deviate from the shortest path can reaccess it [e.g., through brief (one-step) excursions or detours], captured by path transitivity $M(\pi_{s \to t})$, may influence path accessibility (Fig. 1*D*). Overall, these measures predict that paths with stronger edge weights (shorter weighted path length), involving fewer steps,

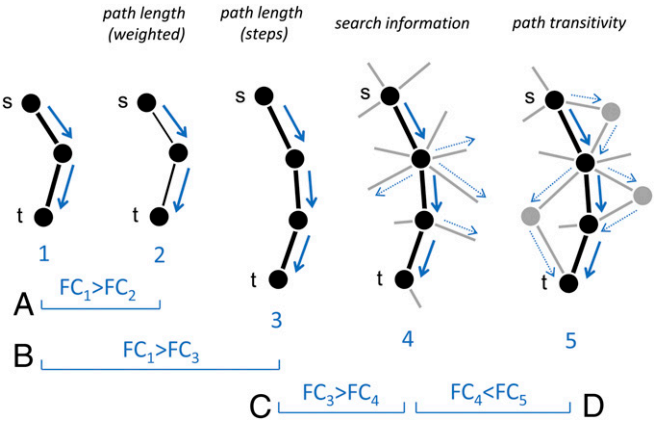

Fig. 1. Schematic diagram of network measures. A source node "s" is linked to a target node "t" by a shortest path (black nodes and edges), embedded in the rest of the network (gray nodes and edges). Connection weight is proportional to line width. The arrows indicate the direction of communication along the shortest path (solid arrows) or away from it (dotted arrows). (*A*) Stronger weights along the path predict FC1 > FC2. (*B*) More steps along the path predict FC1 > FC3. (*C*) Lower node degree along the path (lower search information) predicts FC3 > FC4. (*D*) Fewer local detours along the path (lower path transitivity) predict FC4 < FC5.

with lower-degree nodes along the way and more local detours should promote more efficient communication and hence result in higher FC.

Prediction of FC

Three high-resolution datasets (labeled LAU1, LAU2, and UTR; *SI Methods*) recording networks of structural and functional connections between ~1,000 parcels of human cerebral cortex were used for constructing and testing computational models. SC was inferred on the basis of diffusion imaging [diffusion spectrum imaging (DSI) for LAU1 and LAU2; diffusion tensor imaging for UTR] and tractography; resting-state FC was measured as Pearson cross-correlations between fMRI time series recorded for periods totaling 35 min (LAU1), 9 min (LAU2), and 8 min (UTR). Despite differences in imaging sites, data acquisition, preprocessing, and participant cohorts, group-averaged structural and functional connection matrices displayed significant statistical relationships across all datasets (Fig. S1). Confirming and extending previous studies (2, 11), the strength of structural connections among connected node pairs was significantly correlated with the strength of the corresponding functional connections ($\hat{R} = 0.515$ for 66 anatomical regions; $\hat{R} = 0.338$ for high-resolution matrices). The symbol $\hat{R}$ denotes an average of correlation values across all three datasets. All correlation P values reported in this study are $P < 0.001$.

In accordance with previous reports (11), functional connections between structurally connected node pairs were on average significantly stronger than functional connections between unconnected node pairs (Fig. 2*A*, all $P < 0.001$), and the strength of FC among node pairs declined with their spatial separation estimated as the Euclidean distance (Fig. 2*B*). In each distance bin, FC between structurally connected pairs was significantly stronger than between unconnected pairs (all $P < 0.001$). The strength of functional connections declined with the length of the shortest path, expressed as the number of steps (Fig. 2*C*). Jointly, these observations suggest that connectedness, physical distance, and path length are partially predictive of the strength of FC.

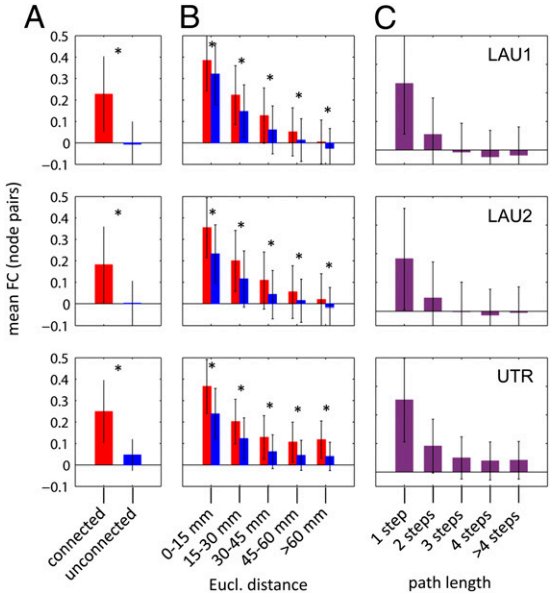

Fig. 2. Relation of empirical FC to connectedness, Euclidean distance, and path length, across three datasets (LAU1, top row; LAU2, middle row; UTR, bottom row). (*A*) Mean ± SD of pairwise FC, averaged over node pairs that are structurally connected (red) and structurally unconnected (blue). (*B*) Pairwise FC, averaged over connected (red) and unconnected (blue) node pairs in relation to their Euclidean distance. (*C*) Pairwise FC, averaged over all node pairs, in relation to path length (number of steps), computed on the SC matrix. The asterisk (*) denotes significant differences (independent-sample t test, $P < 0.01$) between connected and unconnected pairs.

Group-averaged SC was used in simulations of nonlinear neural mass models (11, 17; see *SI Methods*) as well as analytic linear models (30). These models generated patterns of cross-correlations that were significantly correlated with those recorded empirically (Fig. S2 *A* and *B*), and hence succeeded in partially predicting FC from SC. In neural mass models, correlations between simulated FC and empirical FC were examined across a range of coupling strengths (Fig. S2*C*), with peak correlations at $\hat{R} = 0.423$, $\hat{R} = 0.359$, and $\hat{R} = 0.251$, for all node pairs, structurally connected pairs and structurally unconnected pairs in the right cerebral hemisphere (RH), respectively (see Table S1 for performance on individual datasets). FC prediction was consistently found to be stronger for node pairs within the same cortical hemisphere than for node pairs across the whole brain, likely due to incomplete capture of cross-hemispheric SC pathways. In linear models (see *SI Methods*), the corresponding levels of correlations between simulated and empirical FC were $\hat{R} = 0.391$, $\hat{R} = 0.266$, $\hat{R} = 0.216$ (RH; all, connected, unconnected pairs; Table S1). The Euclidean distance between node pairs has been used previously as a predictor of FC (19). Across the three datasets, a linear regression model of FC based on Euclidean distance, derived from the spatial positions of individual cortical parcels, yielded $\hat{R} = 0.419$, $\hat{R} = 0.584$, and $\hat{R} = 0.330$ (RH; all, connected, unconnected pairs; Table S1).

To compare the capacity of analytic measures of network communication to predict empirically measured FC, we derived a series of linear regression models. Table S1 summarizes regression coefficients obtained from four predictors, comprising the weighted path length (D), the path length expressed as the number of steps (K), the search information (S), and the path transitivity (M), all derived from weighted group-averaged SC matrices. The capacity of these predictors was robust with respect to the choice of the weight-to-distance transform used to compute the shortest path (compare Tables S1 and S2). For example, regarding search information, using the negative log of the SC to compute the shortest path yielded $\hat{R} = 0.488$, $\hat{R} = 0.443$, and $\hat{R} = 0.315$ (RH; all, connected, unconnected pairs; Table S1), whereas using the inverse of SC yielded $\hat{R} = 0.467$, $\hat{R} = 0.422$, and $\hat{R} = 0.302$ (RH; all, connected, unconnected pairs; Table S2). Ranking the capacity of these four predictors to model empirical FC revealed that predictions on the basis of S and M were comparably strong across all three datasets (single and both hemispheres), and consistently outperformed predictions derived from D and K. For both search information and path transitivity, the strength of the predictive relationship was found to exceed that obtained by computational models of linear or nonlinear brain dynamics, as well as the Euclidean distance. Notably, in contrast to computational models, analytic measures did not require parameter exploration or fitting and their only input consisted of a weighted SC matrix.

Fig. 3*A* shows a matrix of empirically measured FC (LAU1) and corresponding (predictive) matrices of pairwise search information and pairwise path transitivity, both derived analytically from the empirical SC. Fig. 3*B* shows the corresponding scatterplots. Regarding search information, we determined the portion of the correlation that was accounted for by path length. Importantly, across all three datasets, search information remained significantly predictive of FC after regressing out the stepwise path length ($\hat{R} = 0.357$ and $\hat{R} = 0.307$, all pairs; RH, both hemispheres, respectively) and when stratifying data by path length (Fig. 3*C*). This implies that, given an equal number of steps, FC among node pairs is stronger if the shortest path is more accessible (Fig. 1*C*). Regarding path transitivity, the measure remains predictive of empirical FC across node pairs separated by a path length of one step even after regressing out the effect of search information. The result suggests that for short paths that are equally accessible more local detours along the path tend to yield higher empirical FC

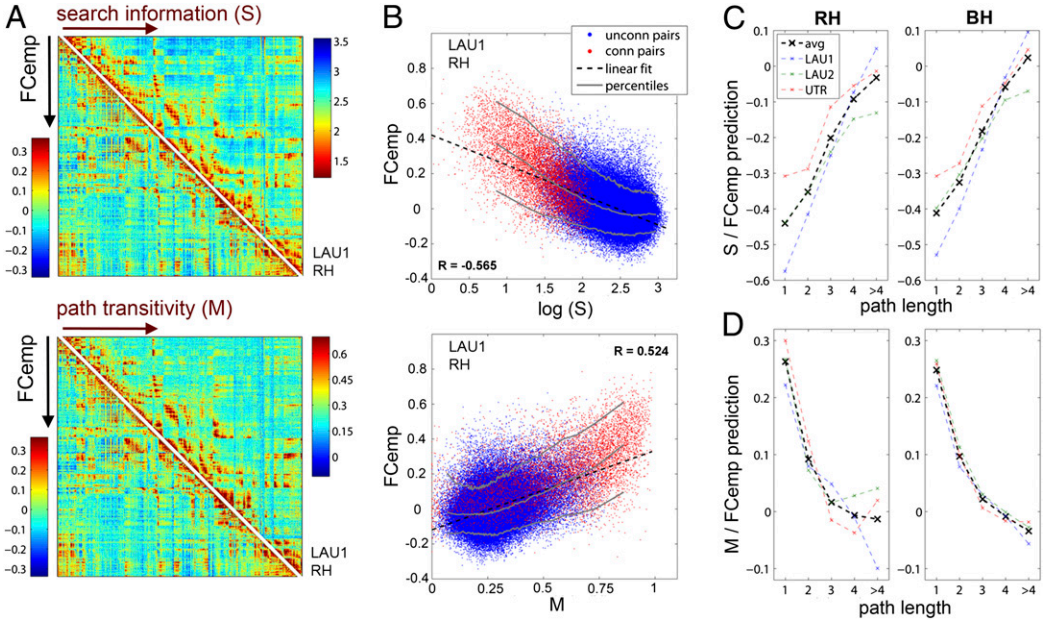

Fig. 3. Predicting empirical FC with search information and path transitivity. (*A*) Pattern of FCemp (lower matrix triangle) and *S* (upper plot, upper matrix triangle) as well as *M* (lower plot, upper matrix triangle) in dataset LAU1 RH. These and all other matrix plots in this paper are scaled to range from −3 SD to +3 SD. Node ordering follows an anatomical progression from frontal to parietal, occipital, and temporal lobes. (*B*) Corresponding scatter plot of *S* vs. FCemp (*Upper*) and *M* vs. FCemp (*Lower*), with red dots indicating structurally connected node pairs, and blue dots indicating structurally unconnected node pairs. The dashed black line indicates the linear fit, and the gray lines indicate the 10th, 50th, and 90th percentiles of FCemp along binned predictors [log(*S*) and *M*]. (*C*) Strength of *S*/FCemp prediction for paths of equal length. (*D*) Strength of *M*/FCemp prediction, after regression on log(*S*), for paths of equal length.

(Fig. 1*D*). The effect diminishes rapidly as path lengths increase (Fig. 3*D*).

A joint multilinear model comprising all four communication-based predictors yielded robust prediction accuracy across all datasets (Table S1, Fig. 4 *A* and *B*, and Fig. S3). Despite partial collinearity between individual predictors (Fig. S4), each predictor in all datasets contributed significantly to the overall multilinear model (all $P < 10^{-6}$). The prediction was strongest for the dataset with the longest fMRI acquisition time (LAU1), reaching $R = 0.598$ across all RH node pairs. Notably, prediction of FC was strong and significant across both structurally connected ($R = 0.616$) and structurally unconnected node pairs ($R = 0.403$). Multilinear models of analytic predictors consistently outperformed the Euclidean distance as well as linear and nonlinear neural models (Tables S1 and S2). When computing nodewise predictions of FC, there was a strong correlation between the analytic multilinear model and the nonlinear neural mass model (Fig. S5). This indicates that the two models tend to perform equally well or equally poorly across regions of the cortex, possibly pointing to imperfections in the SC matrix as a common factor that limits model performance. Indeed, progressive randomization of the SC matrix resulted in lower prediction accuracy (Fig. S6). Fig. S7 shows examples of seed-based correlation patterns mapped onto the cortical surface, allowing visual comparison of empirical FC and predicted FC (multilinear model; dataset LAU1).

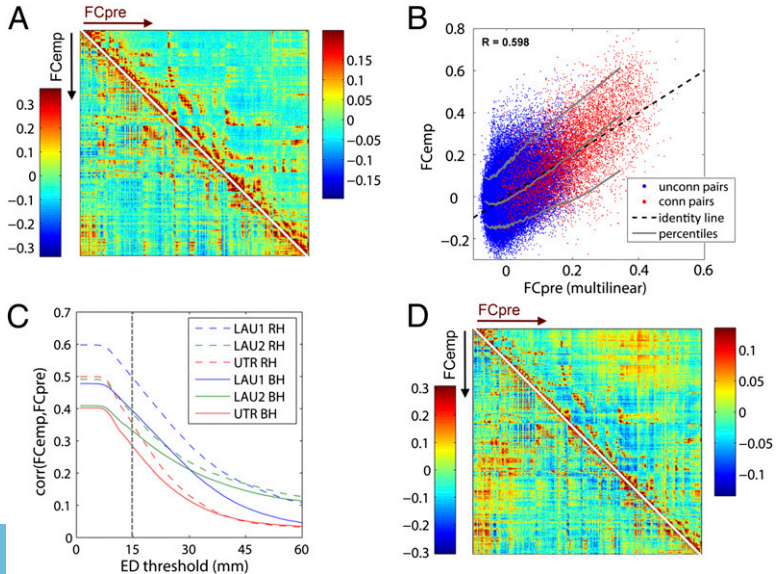

Fig. 4. Multilinear model prediction and its dependence on Euclidean distance (ED). (*A*) Pattern of FCemp (lower matrix triangle) and FC prediction (FCpre) derived from a multilinear model combining all four predictors (upper matrix triangle) in dataset LAU1, right hemisphere. Plots corresponding to multilinear predictions from all datasets are shown in Fig. S3. (*B*) Corresponding scatter plot, with the dashed black line indicating identity, and the gray lines indicating the 10th, 50th, and 90th percentiles of FCemp. (*C*) Effect of thresholding away node pairs separated by short ED on the correlation between FCemp and FCpre. (*D*) Pattern of FCemp residuals after regression on ED (lower matrix triangle) and FC prediction derived from a multilinear model combining all four predictors after regression on ED (upper matrix triangle) in dataset LAU1, right hemisphere.

To better assess the influence of distance effects, including possible distance biases in imaging methodology, on the ability of communication measures to predict FC, we performed two additional analyses. Fig. 4*C* plots the prediction accuracy of the multilinear model as a function of a distance threshold, below which node pairs were omitted from the prediction. Although FC prediction drops as the threshold is raised, it remains strong and significant when short-distance relationships (e.g., <15 mm) are removed. In another analysis, the Euclidean distance was fully regressed out from all communication-based predictors as well as from the empirical FC. After regression, multilinear models continued to yield significant prediction accuracy, across all datasets and weight-to-distance transforms (Tables S1 and S2). This suggests that the capacity of analytic measures of communication to predict empirical FC cannot be accounted for by a relationship of these measures and of FC with Euclidean distance.

To test for cross-model prediction, we substituted, for each dataset, model coefficients from the other datasets and recomputed the predicted FC matrix. Prediction accuracy remained high (Table S3) for all substitutions, indicating robustness of the model parameters across datasets.

Discussion

Dynamic fluctuations of neural signals in the resting brain generate patterns of FC that exhibit characteristic topography when measured with fMRI (5, 6). When recorded over long time periods, this spatial patterning of FC provides important information about the functional organization of intrinsic or resting-state networks (31, 32). The generative mechanisms that shape FC patterns and that can account for significant variations across healthy individuals and across disease states are therefore of great interest. The present paper explored the capacity of analytic measures that capture the network embedding of shortest paths, derived from the SC matrix, to predict FC. These measures, singly or in conjunction, were found to predict the strength of FC among both connected and unconnected node pairs, at levels that matched or significantly exceeded more conventional path length measures, Euclidean distance, as well as computational models of neural dynamics.

Understanding the relationship between SC (the sparse network of axonal links among brain regions) and FC (the dense network of statistical couplings among their neural time series) remains a central challenge for computational cognitive neuroscience. Empirical studies have demonstrated a robust relationship between anatomical networks and networks of dynamic couplings at the macroscale of whole-brain activity (4, 11–13), the mesoscale of intraareal and interareal connectivity (14), as well as the microscale of neuronal circuits (33). Computational studies have built on these empirical data and delivered models of structurally constrained and endogenously driven neural dynamics that can reproduce key features of observed FC (11, 17, 18). Here, we addressed the relation between SC and FC by defining and assessing analytic measures of network communication. This approach is valuable because the degree to which these measures can predict FC may provide conceptual insight into aspects of dynamic interactions along structural connections among brain regions. Notably, the approach creates explicit links between communication processes unfolding within the SC matrix and the emergent pattern of FC, rather than relying on a phenomenological description of FC alone.

In applications of graph theory to brain networks most studies have focused on shortest paths as the principal routes along which communication unfolds (22). Indeed, it seems plausible that interactions along such paths are dynamically favored (faster and less prone to noisy interference). However, accessing shortest paths requires information (25–27, 34, 35), due to the availability of vast numbers of less efficient alternatives. Hence, the contributions of shortest paths to neuronal communication should depend at least in part on how these paths are embedded within the global network. To capture some of the factors that promote dynamic interactions along shortest paths, we developed two measures that supplement the more standard measure of shortest path length (measured as either weighted distance or number of steps) by taking into account how such paths are embedded in the rest of the network (Fig. 1).

Search information quantifies the degree to which the shortest, and presumably most efficient, communication path is hidden within the network (25–27), here adapted for weighted networks. Our principal findings were that search information predicted FC more strongly than path length alone, and that it remained predictive even when considering pairs of regions separated by an equal number of steps. This suggests a significant role of the (weighted) degree sequence associated with the path: the more connections are attached to nodes along the shortest path, the lower the strength of FC (Fig. 1*C*). At least two explanations could account for this effect, one due to congestion or noise at "busier" nodes, and the other due to greater dispersion of signals along the path. A corollary of our findings regarding search information is that communication paths that travel across high-degree nodes, e.g., those comprising the brain's rich club (36, 37), although topologically efficient due to short path length, may incur a cost as high-degree nodes impose higher search information and thus attenuate the strength of FC.

Path transitivity, defined here for undirected weighted networks, is computed as the average pairwise matching index, capturing the density of local detours along the path. Essentially, high path transitivity implicates the existence of many closed loops involving nodes along the path, and dynamically these closed loops may counteract the potential for signal dispersion measured by search information. We found that path transitivity was a strong predictor of FC, equal in strength to search information, and that more local detours promote stronger FC (Fig. 1*D*). Possible explanations involve increased common input onto nodes along the path, feedback loops that recurrently stabilize signals, or recapturing of signals that have gone "off-path." The lack of directionality in human diffusion data precludes distinguishing these alternatives, but the question could be addressed in directed connectivity data from nonhuman primates. A corollary of our findings regarding path transitivity is that communication paths that use nodes with high matching index, such as those interconnected in dense subnetworks or modules, boost FC.

The capacity of search information and path transitivity along shortest paths to predict whole-brain FC may provide some conceptual insight about the nature of the underlying communication process. If communication operates under a perfect routing policy, the degree to which the shortest path is hidden should be irrelevant to the efficiency by which signals propagate, because alternative (and less efficient) paths are excluded from access. In other words, perfect routing predicts no relationship between search information or path transitivity and the strength of FC. The fact that we observe such a relationship implies that neuronal interactions during spontaneous or resting-brain dynamics are not fully accounted for by perfect routing models and instead suggest diffusion or spreading dynamics (35, 38) or "greedy routing" strategies (37) as potential candidate models for brain network communication. Specifically, our results demonstrate that the embedding of shortest paths within the network plays an additional important role, in particular the (weighted) degree sequence of the path and the availability of detours.

Other generative models for FC have been proposed, focusing on the role of spatial distance along with simple topological measures (19, 39) and critical dynamics (20, 21). A generative model based on the competition between a distance penalty and a tendency to link regions with matching inputs was able to reproduce key features of empirical resting fMRI FC (19). Our findings point to a similar trade-off between the effects of network communication measures on FC. An important difference is that our measures are derived from the SC matrix, and that search information and path transitivity account for attributes of shortest paths that depend on the network context within which the path is embedded. Another generative model was based on

an analytically solvable Ising-spin attractor (20) and, in a low-resolution version of the LAU1 dataset, demonstrated overlap between the empirical and modeled FC at a global SC coupling strength that places the system near a critical bifurcation point. The relationship between these near-critical dynamics and the network measures explored in the present study remains to be investigated in future work.

Although the modeling approach presented in this paper has potential advantages, it also has limitations. One limitation is that analytic measures only predict the long-time covariance structure of communication processes unfolding on the SC matrix but cannot account for time-varying or nonstationary couplings (8, 9), dynamic phenomena like noisy fluctuations around marginally stable states (18, 21), or more complex measures of FC involving nonlinear coupling or partial correlation. Another limitation is that the model explored here assumes that FC is exclusively due to communication along shortest paths within the network, and excludes other factors that can boost FC, e.g., alternative (longer) paths, common input, or state-dependent modulation. Finally, model performance is subject to limitations inherent in neuroimaging data acquisition. These limitations include lack of directionality in SC, the quality of diffusion imaging data and the tractography reconstructions of fiber pathways, and run lengths and appropriate denoising of resting-state fMRI. Although our results are robust across three different datasets with varying acquisition parameters and techniques, the approach pursued in this paper will benefit from future methodological refinements that further improve sensitivity, spatial and temporal resolution. Further extensions include FC prediction within single subjects as well as use of data-driven (as opposed to atlas-based or random) parcellation schemes.

With these limitations in mind, we conclude that analytic graph-based measures of network communication are capable of predicting patterns of resting-brain FC. Our findings lend support to the idea that, to a large extent, the long-time average of resting-brain FC is shaped by the underlying SC, thus supporting a causal role of the connectome in generating characteristic attributes of the brain's functional organization.

Materials and Methods

Details on experimental materials and methods are presented in *SI Materials and Methods*. In summary, datasets consisted of group-averaged, high-resolution structural and functional connectivity matrices describing connections of human cerebral cortex (see *SI Materials and Methods, Datasets*). Prediction of functional connectivity from structural connectivity was analyzed in simulations of linear models (30; see *SI Materials and Methods, Linear Model*) and nonlinear neural models (11, 17; see *SI Materials and Methods, Neural Mass Model*). Results were compared to predictions based on analytic measures of network communication, as described in the main text.

ACKNOWLEDGMENTS. We thank Chris Honey for valuable suggestions. J.G. and O.S. were supported by the J. S. McDonnell Foundation. R.F.B. was supported by the National Science Foundation/Integrative Graduate Education and Research Traineeship Training Program in the Dynamics of Brain–Body–Environment Systems at Indiana University. M.P.v.d.H. was supported by Netherlands Organization for Scientific Research Grant VENI-451-12-001 and a fellowship of the Brain Center Rudolf Magnus. A.G. was supported by the Swiss National Science Foundation (Schweizerische Nationalfonds Grant 320030-130090). P.H. was supported by the Leenaards Foundation. B.C.-M. was supported by the Austrian Fonds zur Förderung der Wissenschaftlichen Forschung Project "Quantifying Socioeconomic Multiplex Networks in a Massive Multiplayer Online Game" KPP23378FW.

1. Sporns O, Tononi G, Kötter R (2005) The human connectome: A structural description of the human brain. *PLoS Comput Biol* 1(4):e42.
2. Hagmann P, et al. (2008) Mapping the structural core of human cerebral cortex. *PLoS Biol* 6(7):e159.
3. Iturria-Medina Y, Sotero RC, Canales-Rodríguez EJ, Alemán-Gómez Y, Melie-García L (2008) Studying the human brain anatomical network via diffusion-weighted MRI and Graph Theory. *Neuroimage* 40(3):1064–1076.
4. Gong G, et al. (2009) Mapping anatomical connectivity patterns of human cerebral cortex using in vivo diffusion tensor imaging tractography. *Cereb Cortex* 19(3): 524–536.
5. De Luca M, Beckmann CF, De Stefano N, Matthews PM, Smith SM (2006) fMRI resting state networks define distinct modes of long-distance interactions in the human brain. *Neuroimage* 29(4):1359–1367.
6. Fox MD, et al. (2005) The human brain is intrinsically organized into dynamic, anticorrelated functional networks. *Proc Natl Acad Sci USA* 102(27):9673–9678.
7. Smith SM, et al. (2009) Correspondence of the brain's functional architecture during activation and rest. *Proc Natl Acad Sci USA* 106(31):13040–13045.
8. Chang C, Glover GH (2010) Time-frequency dynamics of resting-state brain connectivity measured with fMRI. *Neuroimage* 50(1):81–98.
9. Buldyrev SV, Parshani R, Paul G, Stanley HE, Havlin S (2010) Catastrophic cascade of failures in interdependent networks. *Nature* 464(7291):1025–1028.
10. Vincent JL, et al. (2007) Intrinsic functional architecture in the anaesthetized monkey brain. *Nature* 447(7140):83–86.
11. Honey CJ, et al. (2009) Predicting human resting-state functional connectivity from structural connectivity. *Proc Natl Acad Sci USA* 106(6):2035–2040.
12. van den Heuvel MP, Mandl RCW, Kahn RS, Hulshoff Pol HE (2009) Functionally linked resting-state networks reflect the underlying structural connectivity architecture of the human brain. *Hum Brain Mapp* 30(10):3127–3141.
13. Hermundstad AM, et al. (2013) Structural foundations of resting-state and task-based functional connectivity in the human brain. *Proc Natl Acad Sci USA* 110(15):6169–6174.
14. Wang Z, et al. (2013) The relationship of anatomical and functional connectivity to resting-state connectivity in primate somatosensory cortex. *Neuron* 78(6):1116–1126.
15. Johnston JM, et al. (2008) Loss of resting interhemispheric functional connectivity after complete section of the corpus callosum. *J Neurosci* 28(25):6453–6458.
16. Adachi Y, et al. (2012) Functional connectivity between anatomically unconnected areas is shaped by collective network-level effects in the macaque cortex. *Cereb Cortex* 22(7):1586–1592.
17. Honey CJ, Kötter R, Breakspear M, Sporns O (2007) Network structure of cerebral cortex shapes functional connectivity on multiple time scales. *Proc Natl Acad Sci USA* 104(24):10240–10245.
18. Deco G, Jirsa VK, McIntosh AR (2011) Emerging concepts for the dynamical organization of resting-state activity in the brain. *Nat Rev Neurosci* 12(1):43–56.
19. Vértes PE, et al. (2012) Simple models of human brain functional networks. *Proc Natl Acad Sci USA* 109(15):5868–5873.
20. Deco G, Senden M, Jirsa V (2012) How anatomy shapes dynamics: A semi-analytical study of the brain at rest by a simple spin model. *Front Comput Neurosci* 6:68.
21. Deco G, et al. (2013) Resting-state functional connectivity emerges from structurally and dynamically shaped slow linear fluctuations. *J Neurosci* 33(27):11239–11252.
22. Latora V, Marchiori M (2001) Efficient behavior of small-world networks. *Phys Rev Lett* 87(19):198701.
23. Easley D, Kleinberg J (2010) *Networks, Crowds, and Markets* (Cambridge Univ Press, Cambridge, UK).
24. El Gamal A, Kim YH (2011) *Network Information Theory* (Cambridge Univ Press, Cambridge, UK).
25. Sneppen K, Trusina A, Rosvall M (2005) Hide-and-seek on complex networks. *Europhys Lett* 69:853–859.
26. Rosvall M, Grönlund A, Minnhagen P, Sneppen K (2005) Searchability of networks. *Phys Rev E Stat Nonlin Soft Matter Phys* 72(4 Pt 2):046117.
27. Trusina A, Rosvall M, Sneppen K (2005) Communication boundaries in networks. *Phys Rev Lett* 94(23):238701.
28. Corominas-Murtra B, Rodríguez-Caso C, Goñi J, Solé R (2010) Topological reversibility and causality in feed-forward networks. *New J Phys* 12:113051.
29. Hilgetag CC, Burns GA, O'Neill MA, Scannell JW, Young MP (2000) Anatomical connectivity defines the organization of clusters of cortical areas in the macaque monkey and the cat. *Philos Trans R Soc Lond B Biol Sci* 355(1393):91–110.
30. Fernández Galán R (2008) On how network architecture determines the dominant patterns of spontaneous neural activity. *PLoS One* 3(5):e2148.
31. Power JD, et al. (2011) Functional network organization of the human brain. *Neuron* 72(4):665–678.
32. Yeo BTT, et al. (2011) The organization of the human cerebral cortex estimated by intrinsic functional connectivity. *J Neurophysiol* 106(3):1125–1165.
33. Pernice V, Staude B, Cardanobile S, Rotter S (2011) How structure determines correlations in neuronal networks. *PLoS Comput Biol* 7(5):e1002059.
34. Noh JD, Rieger H (2004) Random walks on complex networks. *Phys Rev Lett* 92(11): 118701.
35. Goñi J, et al. (2013) Exploring the morphospace of communication efficiency in complex networks. *PLoS One* 8(3):e58070.
36. van den Heuvel MP, Sporns O (2011) Rich-club organization of the human connectome. *J Neurosci* 31(44):15775–15786.
37. van den Heuvel MP, Kahn RS, Goñi J, Sporns O (2012) High-cost, high-capacity backbone for global brain communication. *Proc Natl Acad Sci USA* 109(28):11372–11377.
38. O'Dea R, Crofts JJ, Kaiser M (2013) Spreading dynamics on spatially constrained complex brain networks. *J R Soc Interface* 10(81):20130016.
39. Alexander-Bloch AF, et al. (2013) The anatomical distance of functional connections predicts brain network topology in health and schizophrenia. *Cereb Cortex* 23(1): 127–138.